

# Control Strategy of OLTC using Quantum Binary Particle Swarm Optimization to Improve the Voltage Stability Index

**Aji Akbar Firdaus**

Institut Teknologi Sepuluh Nopember, Surabaya, Indonesia | Universitas Airlangga, Surabaya, Indonesia  
7022202001@student.its.ac.id

**Adi Soeprijanto**

Institut Teknologi Sepuluh Nopember, Surabaya, Indonesia  
adisup@its.ac.id (corresponding author)

**Ardyono Priyadi**

Institut Teknologi Sepuluh Nopember, Surabaya, Indonesia  
priyadi@its.ac.id

**Dimas Fajar Uman Putra**

Institut Teknologi Sepuluh Nopember, Surabaya, Indonesia  
dimasfup@its.ac.id

Received: 25 November 2024 | Revised: 2 January 2025, 23 January 2025, and 4 February 2025 | Accepted: 6 February 2025

Licensed under a CC-BY 4.0 license | Copyright (c) by the authors | DOI: <https://doi.org/10.48084/etasr.9715>

## ABSTRACT

Efficient voltage regulation in distribution and transmission systems heavily relies on transformers with On-Load Tap Changers (OLTC). This study introduces a novel optimization technique, called Quantum Binary Particle Swarm Optimization (QBPSO), to optimize transformer tap settings to improve voltage stability and reducing power losses. QBPSO combines the principles of quantum computing with binary particle swarm optimization, enhancing the algorithm's exploration and exploitation capabilities. Utilizing the Bus Injection to Branch Current-Branch Current to Bus Voltage (BIBC-BCBV) method for power flow analysis, this research evaluates the performance of the proposed method on the IEEE 34-bus 20 kV radial distribution system. The results indicate a significant reduction in the Voltage Stability Index (VSI) from 0.2257 to 0.2069, a decrease in power losses from 21.756 kW to 19.1573 kW, and an improvement in the average voltage from 19.0047 kV to 19.9453 kV. A comparative analysis with Genetic Algorithm (GA), Binary Particle Swarm Optimization (BPSO), and Quantum Differential Evolution (QDE) demonstrates that QBPSO achieves superior performance in computational efficiency and voltage stability enhancement. These results highlight the effectiveness of QBPSO as a powerful tool for optimizing OLTC settings, contributing to the reliability and efficiency of power distribution systems.

**Keywords**-BIBC-BCBV; distribution network; OLTC; QBPSO; VSI

## I. INTRODUCTION

Voltage stability and power loss minimization are critical concerns in the operation of electrical distribution networks. As the electricity demand continues to rise, improving the efficiency and reliability of power distribution systems has become increasingly important [1-3]. Voltage instability can lead to blackouts and system failures, so developing strategies that ensure stable and efficient power delivery is essential. An On-Load Tap Changer (OLTC) is a key method to minimize power losses. In [4-8], the application of a static compensator for distribution and voltage regulation on a transformer was

combined with OLTC. Additionally, the control strategy involves coordinating OLTC operations and managing the reactive power exchange from distributed generation and photovoltaic (PV) systems. However, this manual coordination process is time-consuming, and integrating Distributed Generation (DG), wind turbines, and PV systems entails significant costs. Furthermore, variations in load changes and additions further complicate the scenario. To address these challenges, several Artificial Intelligence (AI) methods have been proposed to optimize OLTC. In [9, 10], OLTC was applied for distribution and voltage regulation. These methods

employ various metaheuristic and evolutionary algorithms, including the Genetic Algorithm (GA), Binary Genetic Algorithm (BGA), Particle Swarm Optimization (PSO), Quantum Differential Evolution (QDE), and Binary Particle Swarm Optimization (BPSO), aiming to minimize power losses.

The use of PSO in optimization has been extensively explored, particularly in the context of OLTC. In PSO, particles represent potential solutions and move through the solution space following the best-performing particles. This collective behavior helps the swarm to converge to optimal solutions efficiently. However, PSO is prone to local minima and parameter sensitivity issues, making it less effective for discrete optimization problems [11]. To overcome these limitations, BPSO has been developed specifically for discrete function optimization. BPSO modifies the standard PSO by constraining particle positions to binary values, making it suitable for problems with binary decision variables [12]. Despite its advantages, BPSO has limitations. One notable weakness lies in its initial randomization process, which can result in suboptimal solutions. The randomization of binary particles in BPSO can sometimes hinder the effective exploration of the solution space, thus affecting the algorithm's ability to converge towards the global optimum [13]. This limitation necessitates further enhancements to improve the algorithm's performance in complex optimization tasks. Recent advances include Quantum Particle Swarm Optimization (QPSO), which enhances optimization capabilities by integrating quantum computing principles [14-16]. Quantum computing introduces concepts such as superposition and entanglement, allowing for a more comprehensive exploration of the solution space.

This paper introduces QBPSO to optimize OLTC settings in distribution networks, aiming to enhance voltage stability and minimize power losses. The proposed method was evaluated on the IEEE 34-bus 20 kV radial distribution system. The results indicate significant improvements in voltage stability and reductions in power losses, demonstrating the effectiveness of QBPSO in enhancing the efficiency and reliability of power distribution systems.

## II. RESEARCH METHOD

The implementation of QBPSO for controlling an OLTC starts by initializing the particles within the QBPSO framework. Each particle represents a potential solution for the OLTC's tap settings, with initial positions and velocities set within defined limits to explore feasible solutions. Once initialized, the fitness of each particle is evaluated according to predefined criteria, such as the voltage stability index or power loss reduction, which reflect the performance of the voltage profile across the distribution system. After fitness evaluation, the algorithm updates each particle's personal best ( $p_{best}$ ) and global best ( $g_{best}$ ) values. Specifically, if a particle's current fitness is better than any previous fitness value it achieved, its position updates to  $p_{best}$ . Similarly, if a particle's fitness surpasses the best fitness identified by the entire swarm,  $g_{best}$  updates to this new optimal position.

The next step involves adjusting each particle's velocity and position using the QBPSO formula, which incorporates a stochastic quantum component to enhance search space exploration. This quantum-inspired update ensures that particles explore a broader range of potential solutions, which aids in escaping local optima. Finally, convergence is assessed by determining whether the algorithm meets the iteration limit or if  $g_{best}$  stabilizes with minimal changes over subsequent iterations. If the convergence criteria are not met, the algorithm loops back to fitness evaluation, iterating until the optimal solution for OLTC control is achieved.

### A. Formulation of the Problem in the Radial Distribution System

The primary objective is to reduce the Voltage Stability Index (VSI), an essential metric for evaluating the voltage stability level across an interconnected power system. A lower VSI indicates better system stability, with optimal stability achieved when VSI approaches zero [17-19]. The VSI in the two-bus equivalent model of the distribution system is illustrated in Figure 1.  $P_i$ ,  $Q_i$ , and  $V_i$  represent the sending-end of total active power, reactive power, and voltage, respectively. Similarly,  $P_{i+1}$ ,  $Q_{i+1}$ , and  $V_{i+1}$  denote the receiving-end active power, reactive power, and voltage.  $r_i + jx_i$  represents the data of the line between the sending bus and the receiving bus.

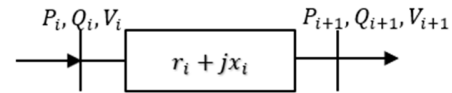


Fig. 1. The two-bus equivalent model of the distribution system.

From the system modeling shown in Figure 1, the line current equations for the two-bus system can be calculated using (1) and (2).  $P_L$  and  $Q_L$  refer to the active and reactive power losses of the distribution line, respectively.

$$I^2 = \frac{P_{i+1}^2 + Q_{i+1}^2}{V_{i+1}^2} \quad (1)$$

$$I^2 = \frac{(P_L^2 + Q_L^2)}{(V_i - V_{i+1})^2} \quad (2)$$

From (1) and (2), (3) is obtained.

$$\frac{P_{i+1}^2 + Q_{i+1}^2}{V_{i+1}^2} = \frac{(P_L^2 + Q_L^2)}{(V_i - V_{i+1})^2} \quad (3)$$

Then,  $P_L$  and  $Q_L$  can be obtained from (6) and (7).

$$P_i = P_L + P_{i+1} \quad (4)$$

$$Q_i = Q_L + Q_{i+1} \quad (5)$$

$$P_L = r_i \left( \frac{P_{i+1}^2 + Q_{i+1}^2}{V_{i+1}^2} \right) \quad (6)$$

$$Q_L = x_i \left( \frac{P_{i+1}^2 + Q_{i+1}^2}{V_{i+1}^2} \right) \quad (7)$$

Equations (6) and (7) are substituted into (3).

$$(V_i V_{i+1} - V_{i+1}^2)^2 = (P_{i+1}^2 + Q_{i+1}^2) \cdot (r_i^2 + x_i^2) \quad (8)$$

$$V_{i+1}^2 - V_i V_{i+1} + \sqrt{(P_{i+1}^2 + Q_{i+1}^2) \cdot (r_i^2 + x_i^2)} = 0 \quad (9)$$

Equation (10) represents the root calculation of (9).

$$V_i^2 - 4 \cdot \sqrt{(P_{i+1}^2 + Q_{i+1}^2) \cdot (r_i^2 + x_i^2)} \geq 0 \quad (10)$$

$$-4 \cdot \sqrt{(P_{i+1}^2 + Q_{i+1}^2) \cdot (r_i^2 + x_i^2)} \geq -V_i^2 \quad (11)$$

$$4 \cdot \sqrt{\frac{(P_{i+1}^2 + Q_{i+1}^2) \cdot (r_i^2 + x_i^2)}{V_i^2}} \leq 1 \quad (12)$$

From (12), VSI is shown in (13).

$$L_i = 4 \cdot \sqrt{\frac{(P_{i+1}^2 + Q_{i+1}^2) \cdot (r_i^2 + x_i^2)}{V_i^2}} \quad (13)$$

The system's stability level can be evaluated using (13). If  $L_i$  approaches one, the system is considered less stable. Conversely, if  $L_i$  approaches zero, the system is considered more stable [20].

The development of the VSI applied to a two-bus equivalent system derived from a multi-bus system can be illustrated as shown in Figure 2. The total active and reactive power of the load in the two-bus system can be represented by the symbols  $P_R$  and  $Q_R$ , while the total active and reactive power of generation can be represented by  $P_S$  and  $Q_S$ . Consequently, the equivalent impedance is expressed as  $r_{eq}$  and  $x_{eq}$ . The value of the equivalent impedance is obtained through calculations using (16) and (17).

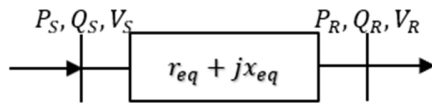


Fig. 2. The two-bus equivalent system.

From (6) and (7), the development equations of the VSI are obtained as shown in (14) and (15).

$$P_L = r_{eq} \left( \frac{P_S^2 + Q_S^2}{V_S^2} \right) \quad (14)$$

$$Q_L = x_{eq} \left( \frac{P_S^2 + Q_S^2}{V_S^2} \right) \quad (15)$$

If  $V_S$  is 1.0 per unit (p.u) because it is close to the generation, then the equation  $r_{eq} + x_{eq}$  can be expressed as:

$$r_{eq} = \left( \frac{P_L}{P_S^2 + Q_S^2} \right) \quad (16)$$

$$x_{eq} = \left( \frac{Q_L}{P_S^2 + Q_S^2} \right) \quad (17)$$

The development of the VSI applied to a two-bus equivalent system derived from a multi-bus system can be represented as (18) [20], assuming  $V_S$  is 1.0 p.u.

$$L = 4 \cdot \sqrt{(P_S^2 + Q_S^2) \cdot (r_{eq}^2 + x_{eq}^2)} \quad (18)$$

### B. Power Flow Analysis in the Radial Distribution System

Power flow analysis in radial distribution systems differs from that in transmission systems. This radial configuration, characterized by a single path between two nodes, requires specialized methods for accurate power flow calculations. One

effective approach for this is the Bus Injection to Branch Current-Branch Current to Bus Voltage (BIBC-BCBV) method, which is particularly well-suited for radial systems [21].

$$\begin{bmatrix} B_1 \\ B_2 \\ B_3 \\ B_4 \\ B_5 \end{bmatrix} = \begin{bmatrix} 1 & 1 & 1 & 1 & 1 \\ 0 & 1 & 1 & 1 & 1 \\ 0 & 0 & 1 & 1 & 0 \\ 0 & 0 & 0 & 1 & 0 \\ 0 & 0 & 0 & 0 & 1 \end{bmatrix} \begin{bmatrix} I_2 \\ I_3 \\ I_4 \\ I_5 \\ I_6 \end{bmatrix} \quad (19)$$

$$[B] = [BIBC][I] \quad (20)$$

From (19), the BCBV matrix can be organized similarly, as shown in (21).

$$\begin{bmatrix} V_1 - V_2 \\ V_1 - V_3 \\ V_1 - V_4 \\ V_1 - V_5 \\ V_1 - V_6 \end{bmatrix} = \begin{bmatrix} Z_{12} & 0 & 0 & 0 & 0 \\ Z_{12} & Z_{23} & 0 & 0 & 0 \\ Z_{12} & Z_{23} & Z_{34} & 0 & 0 \\ Z_{12} & Z_{23} & Z_{34} & Z_{45} & 0 \\ Z_{12} & Z_{23} & 0 & 0 & Z_{36} \end{bmatrix} \begin{bmatrix} B_1 \\ B_2 \\ B_3 \\ B_4 \\ B_5 \end{bmatrix} \quad (21)$$

The general structure of (21) can be formulated similarly to:

$$[\Delta V] = [BCBV][B] \quad (22)$$

If (20) is substituted into (21), the following equation for the voltage drop ( $\Delta V$ ) is obtained.

$$[\Delta V] = [BCBV][BIBC][I] \quad (23)$$

The determination of the power alteration can be achieved through the calculation of iterative equations given in:

$$I_i^{(k)} = \left( \frac{P_i + jQ_i}{V_i^{(k)}} \right)^* \quad (24)$$

$$[V^k] = [BCBV][BIBC][I^k] \quad (25)$$

$$[\Delta V^{k+1}] = [V_1] - [\Delta V^k] \quad (26)$$

where  $V_1$  to  $V_6$  represent the voltages at bus 1 to bus 6,  $Z$  represents the impedance of lines, and  $k$  denotes the iteration of the load flow calculation.

### C. Quantum Binary Particle Swarm Optimization (QBPSO)

PSO, inspired by the collective intelligence observed in bird flocks and fish schools, was introduced by Kennedy and Eberhart [22-25]. The PSO algorithm utilizes a population of particles that move through the solution space. This collective behavior allows the swarm to converge toward optimal solutions efficiently. The standard formulations of the PSO algorithm are represented by (27) and (28).

$$v_i(t+1) = v_i(t) + c_1 \text{rand} (p_p - x_i(t)) + c_2 \text{rand} (p_g - v_i(t)) \quad (27)$$

$$x_i(t+1) = x_i(t) + v_i(t+1) \quad (28)$$

In BPSO, the updates for  $p_g$  and  $p_p$  within the swarm follow the standard PSO procedure. However, the key difference between PSO and BPSO lies in interpreting velocity. In BPSO, velocity is constrained within the range of [0, 1]. The

particle's new position is determined by (29), while its velocity is defined by (30).

$$v_{ij}(t) = sig(t) = \frac{1}{1+e^{-v_{ij}(t)}} \quad (29)$$

$$x_{ij}(t+1) = \begin{cases} 1 & \text{if } r_{ij} < sig(v_{ij}(t+1)) \\ 0 & \text{otherwise} \end{cases} \quad (30)$$

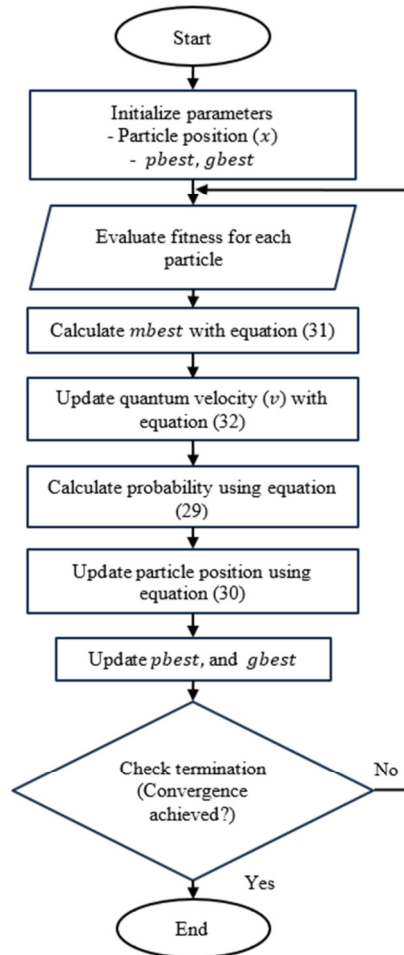


Fig. 3. Flowchart of the proposed method.

QBPSO integrates quantum computing principles with BPSO [26, 27]. It integrates quantum mechanics principles with binary search space optimization to address challenges in discrete optimization problems. QBPSO enhances the exploration-exploitation balance, enabling better convergence and avoiding local optima. Equations (31) and (32) determine the velocity of QBPSO. The parameters  $r_1$ ,  $r_2$ , and  $r_3$  in QBPSO represent random numbers that determine the influence of the personal best ( $p_{best}$ ), global best ( $g_{best}$ ), and mean best ( $m_{best}$ ) positions on particle movement. The values of  $r_1$ ,  $r_2$ , and  $r_3$  are 0.3, 0.4, and 0.3, respectively. The parameters  $\alpha$  and  $\beta$  play a crucial role in achieving a balance between local and global search, effectively guiding the algorithm toward the global optimum without getting trapped in local optima. The parameter  $\alpha$  emphasizes exploration by enabling

particles to search across a broader solution space, preventing premature convergence and allowing the algorithm to discover new and potentially better solutions, while  $\beta$  focuses on exploitation, refining the search within promising regions of the solution space to improve convergence speed toward an optimal solution. The values  $\alpha$  and  $\beta$  are 0.4 and 0.3. The parameter  $N$  is the number of particles. Figure 3 shows the implementation of the QBPSO algorithm.

$$m_{best_j} = \frac{1}{N} \sum_{i=1}^N p_{best_{ij}} \quad (31)$$

$$v_{ij} = \alpha \cdot r_1 \cdot (p_{best_{ij}} - x_{ij}) + \beta \cdot r_2 \cdot (g_{best_j} - x_{ij}) + (1 - \alpha - \beta) \cdot r_3 \cdot (m_{best_j} - x_{ij}) \quad (32)$$

### III. RESULTS AND DISCUSSION

This study used a radial network consisting of 34 buses operating at 20 kV. Figure 4 shows the placement of an OLTC within the IEEE 34-bus system. Detailed line and load data for each bus are presented in Tables I and II, respectively. The load-type column in the bus data table specifies the type of load, with a value of 1 indicating constant power, 2 representing constant current, and 3 denoting constant impedance.

TABLE I. LINE DATA

Branch		Impedance	
From Bus	To Bus	R (Ω)	X (Ω)
1	2	0.6532	0.6518
2	3	0.438	0.4371
3	4	8.1601	8.143
4	5	1.4695	1.4664
4	6	9.4943	9.4744
6	7	7.5271	7.5113
7	8	0.0037	0.0027
8	9	0.1133	0.0829
9	10	0.9067	0.4811
10	11	25.524	13.544
11	12	7.2851	3.8657
9	13	3.7321	2.7294
13	14	0.307	0.2246
13	15	1.6062	0.8525
15	16	7.4714	5.5642
16	17	0.1901	0.139
17	18	12.368	6.5638
17	19	13.462	9.8548
19	20	0.0037	0.0027
20	21	1.7911	1.3099
21	22	0.8588	0.4558
20	23	0.053	0.026
23	24	2.6736	2.668
21	25	2.131	1.5585
25	26	0.1023	0.0749
26	27	0.4935	0.3609
27	28	1.3305	0.9731
28	29	0.1937	0.1417
25	30	0.7384	0.54
30	31	0.9796	0.7164
31	32	0.3144	0.2299
31	33	0.1023	0.0749
33	34	1.7688	1.3082

TABLE II. LOAD DATA

Bus	P (MW)	Q (MVAR)	Load-type
2	0	0	0
3	0	0	0
4	0	0	0
5	0	0	0
6	0	0	0
7	0	0	0
8	0	0	0
9	0	0	0
10	0	0	0
11	0	0	0
12	0	0	0
13	0	0	0
14	0	0	0
15	0	0	0
16	0.01	0.005	3
17	0	0	0
18	0	0	0
19	0	0	0
20	0	0	0
21	0	0	0
22	0	0	0
23	0	0	0
24	0.15	0.075	2
25	0	0	0
26	0	0	0
27	0.135	0.105	3
28	0	0	0
29	0.02	0.016	1
30	0.02	0.016	1
31	0	0	0
32	0.009	0.007	2
33	0	0	0
34	0	0	0

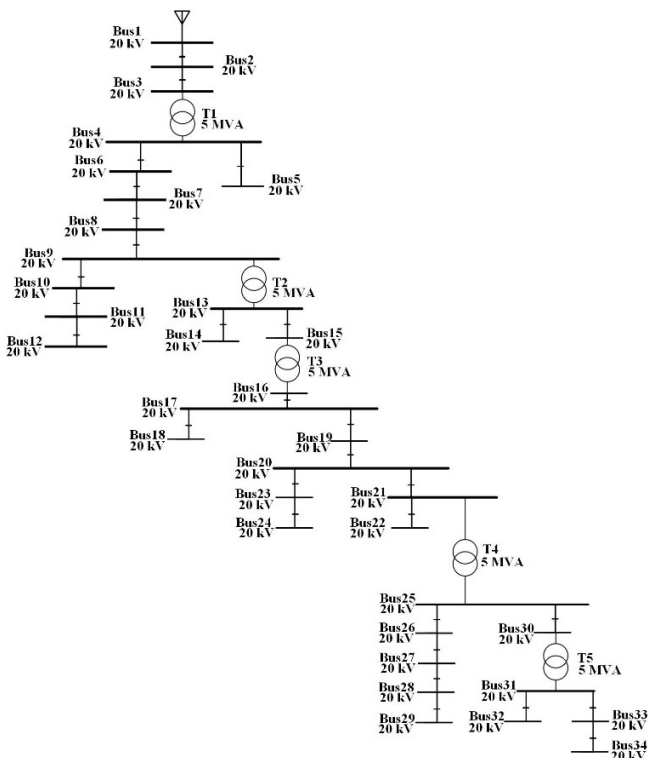


Fig. 4. Distribution system 34-bus.

The radial network consists of 34 buses and five transformers operating at a voltage level of 20 kV, as shown in Figure 4. The transformers are strategically placed between Bus 3 and Bus 4, Bus 9 and Bus 13, Bus 15 and Bus 16, Bus 21 and Bus 25, and Bus 30 and Bus 31. Using the BIBC-BCBV method without OLTC, the power flow analysis results show a total active power load of 428.638 kW and total power losses of 21.756 kW. Additionally, the average voltage is 19.0047 kV, with the lowest voltage recorded at 18.054 kV. These values were obtained from the initial tap settings of transformers 1 to 5, set in the sequence of -1, 0, 2, -1, 0.

TABLE III. RESULTS OF POWER FLOW WITHOUT OLTC COORDINATION

From Bus	To Bus	Current		Losses		Deviation of voltage drop (%)
		I (A)	Angle (deg)	P (kW)	Q (kVAR)	
1	2	20.07	-33.29	0.26	0.26	0.09
2	3	20.07	-33.29	0.18	0.18	0.15
3	4	20.07	-33.29	3.29	3.28	3.79
4	5	0	0	0	0	3.79
4	6	20.07	-33.29	3.82	3.82	5.11
6	7	20.07	-33.29	3.03	3.03	6.16
7	8	20.07	-33.29	0	0	6.16
8	9	20.07	-33.29	0.05	0.03	6.17
9	10	0	0	0	0	6.17
10	11	0	0	0	0	6.17
11	12	0	0	0	0	6.17
9	13	20.07	-33.29	1.5	1.1	6.64
13	14	0	0	0	0	6.64
13	15	20.07	-33.29	0.65	0.34	6.82
15	16	20.07	-33.29	3.01	2.24	7.76
16	17	19.55	-33.46	0.07	0.05	7.78
17	18	0	0	0	0	7.78
17	19	19.55	-33.46	5.14	3.76	9.41
19	20	19.55	-33.46	0	0	9.41
20	21	11.27	-38.58	0.23	0.17	9.54
21	22	0	0	0	0	9.54
20	23	8.39	-26.57	0	0	9.42
23	24	8.39	-26.57	0.19	0.19	9.57
21	25	11.27	-38.58	0.27	0.2	9.69
25	26	9.32	-38.54	0.01	0.01	9.69
26	27	9.32	-38.54	0.04	0.03	9.72
27	28	1.38	-39.2	0	0	9.73
28	29	1.38	-39.2	0	0	9.73
25	30	1.95	-38.82	0	0	9.69
30	31	0.57	-37.87	0	0	9.70
31	32	0.57	-37.87	0	0	9.70
31	33	0	0	0	0	9.70
33	34	0	0	0	0	9.70

Table III presents the power flow analysis for the IEEE 34-bus radial distribution system without OLTC coordination, highlighting key parameters such as current flow, active and reactive power losses, and voltage drops. A significant observation is the line between Bus 3 and Bus 4, which experiences a current of 20.07 A, resulting in active and reactive power losses of 3.29 kW and 3.28 kVAR, respectively. The system's voltage profile, as depicted in Figure 5, reveals that several buses, particularly from Bus 6 to Bus 34, experience voltage drops below the acceptable threshold of ±5% from the base voltage of 20 kV. This indicates areas of voltage instability within the network, reflecting the effects of power losses and inadequate voltage regulation without OLTC

coordination. The lowest recorded voltage is 18.054 kV, underscoring the need for optimization strategies to maintain voltage levels within the allowable ranges and improve overall system stability. Similar inefficiencies are observed across other network parts, highlighting significant power losses and voltage drops without OLTC optimization. These findings establish a basis for evaluating system inefficiencies and highlight the importance of advanced optimization techniques, such as QBPSO, to minimize power losses and enhance voltage stability.



Fig. 5. Profile of Voltage without OLTC coordination.

The optimization simulation of the system using QBPSO aims to achieve optimal OLTC tap coordination, as shown in Table IV, with the objectives of improving voltage stability, minimizing power losses, and maintaining voltage levels within predefined standards. Table V presents the power flow simulation results after OLTC optimization using QBPSO. These findings reveal a total power loss of 19.157 kW and an average voltage of 19.9453 kV. Notably, there are no under-voltage buses, with the minimum voltage recorded at 19.099 kV, as depicted in Figure 6.

Table v presents the power flow analysis results after OLTC optimization using the QBPSO method, highlighting parameters such as current magnitude, active and reactive power losses, and voltage drops for each line in the IEEE 34-bus radial distribution system. These results demonstrate a significant reduction in power losses, with the line between Bus 3 and Bus 4 showing a decrease in active power losses from 3.29 kW to 3.09 kW and reactive power losses from 3.28 kVAR to 3.09 kVAR. Similar improvements were observed across other lines, resulting in enhanced voltage stability and more efficient power distribution. Specifically, this optimization eliminated under-voltage conditions, as all bus voltages are now within the acceptable range of  $\pm 5\%$  from the base voltage of 20 kV, as depicted in Figure 5, with the minimum recorded voltage being 19.099 kV. These findings highlight the effectiveness of QBPSO in minimizing power losses, stabilizing voltage levels, and improving overall system efficiency, making it a valuable tool for optimizing radial distribution networks.

TABLE IV. RESULTS OF OLTC COORDINATION USING QBPSO

Number of Transformers	Tap Transformer	Line Location	
		From Bus	To Bus
1	-1	3	4
2	1	9	13
3	3	15	16
4	-3	21	25
5	3	30	31
5	3	30	31

TABLE V. RESULT OF POWER FLOW WITH OLTC COORDINATION USING QBPSO

From Bus	To Bus	Current		Losses		Deviation of Voltage Drop (%)
		I (A)	Angle (deg)	P (kW)	Q (kVAR)	
1	2	19.47	-33.53	0.25	0.25	0.09
2	3	19.47	-33.53	0.17	0.17	0.15
3	4	19.47	-33.53	3.09	3.09	1.25
4	5	0	0	0	0	1.25
4	6	19.47	-33.53	3.6	3.59	2.53
6	7	19.47	-33.53	2.85	2.85	3.54
7	8	19.47	-33.53	0	0	3.54
8	9	19.47	-33.53	0.04	0.03	3.55
9	10	0	0	0	0	3.55
10	11	0	0	0	0	3.55
11	12	0	0	0	0	3.55
9	13	19.47	-33.53	1.14	0.77	1.50
13	14	0	0	0	0	1.50
13	15	19.47	-33.53	0.61	0.32	1.68
15	16	19.47	-33.53	2.36	1.55	4.92
16	17	18.89	-33.73	0.07	0.05	4.89
17	18	0	0	0	0	4.89
17	19	18.89	-33.73	4.8	3.52	3.32
19	20	18.89	-33.73	0	0	3.32
20	21	11.37	-38.53	0.23	0.17	3.19
21	22	0	0	0	0	3.19
20	23	7.62	-26.57	0	0	3.32
23	24	7.62	-26.57	0.16	0.16	3.18
21	25	11.37	-38.53	0.26	0.03	4.46
25	26	9.51	-38.48	0.01	0.01	4.46
26	27	9.51	-38.48	0.04	0.03	4.49
27	28	1.34	-39.15	0	0	4.50
28	29	1.34	-39.15	0	0	4.51
25	30	1.86	-38.8	0	0	4.47
30	31	0.52	-37.87	0.02	0.02	3.03
31	32	0.52	-37.87	0	0	3.03
31	33	0	0	0	0	3.03
33	34	0	0	0	0	3.03

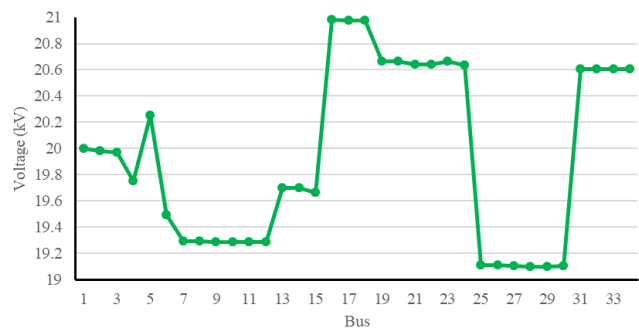


Fig. 6. Voltage profile with OLTC coordination using QBPSO.

Figure 7 illustrates the convergence patterns of GA, QDE, BPSO, and QBPSO. Specifically, GA, QDE, BPSO, and QBPSO reach convergence in the 52nd, 26th, 33rd, and 21st iterations, respectively. Table VI provides a comparative analysis of the performance of GA, BPSO, QDE, and QBPSO in terms of power losses, VSI, and computational time. The power losses observed with the GA are the highest at 19.3016 kW. In contrast, BPSO, QDE, and QBPSO all achieve the same reduced power losses of 19.1573 kW, indicating their superior ability to minimize losses in the system compared to GA. VSI values reflect the voltage stability of the system, with a lower value indicating better stability. GA has the highest VSI at 0.208495035, suggesting lower voltage stability compared to the other algorithms. BPSO, QDE, and QBPSO all achieve a VSI of 0.206936313, demonstrating their effectiveness in improving voltage stability. Computational efficiency is represented by the time taken to converge to an optimal solution. GA is the slowest, taking 15.8789 seconds. BPSO significantly improves this with a time of 10.5559 seconds, followed by QDE at 7.182868 seconds. QBPSO outperforms all other algorithms in terms of speed, requiring only 3.858783 seconds to achieve optimal results. This indicates that QBPSO not only matches BPSO and QDE in minimizing power losses and improving VSI but also does it in a much shorter time frame, highlighting its superior computational efficiency. The table highlights the efficiency and effectiveness of the QBPSO algorithm compared to GA, BPSO, and QDE. QBPSO achieves the lowest power losses and VSI, indicating optimal performance in terms of minimizing losses and enhancing voltage stability. Additionally, QBPSO significantly reduces the computational time required to achieve optimal solutions, demonstrating its superior efficiency and making it the most favorable algorithm for optimizing OLTC settings in the given radial distribution network.

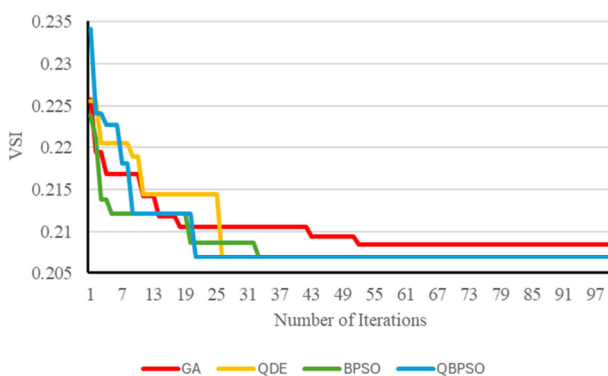


Fig. 7. Convergence comparison of GA, QDE, BPSO, and QBPSO.

TABLE VI. COMPARISON OF RESULTS OF LOSSES, VSI, AND TIME

Algorithm	Losses (kW)	VSI	Time (s)
GA	19.3016	0.208495035	15.8789
BPSO	19.1573	0.206936313	10.5559
QDE	19.1573	0.206936313	7.182868
QBPSO	19.1573	0.206936313	3.858783

#### IV. CONCLUSION

This study demonstrated the effectiveness of the Quantum Binary Particle Swarm Optimization (QBPSO) algorithm in OLTC settings within a 20 kV radial distribution system comprising 34 buses. The implementation of QBPSO significantly reduced active power losses from 21.756 kW to 19.157 kW and improved the average voltage from 19.0047 kV to 19.9453 kV, with the minimum voltage increasing to 19.099 kV, well within the permissible range. QBPSO outperformed other algorithms, such as the Genetic Algorithm (GA), Binary Particle Swarm Optimization (BPSO), and Quantum Differential Evolution (QDE), by achieving a lower VSI of 0.2069 and the fastest computation time of just 3.86 seconds. The optimization results eliminated under-voltage conditions, ensuring that all bus voltages remained within the  $\pm 5\%$  tolerance range. These findings highlight QBPSO's superior capability to enhance voltage stability, reduce power losses, and improve overall system reliability and efficiency. This research provides valuable insights into the application of AI-based optimization methods for modern power distribution systems, offering practical solutions to improve operational quality and sustainability.

#### REFERENCES

- [1] V. K. B. Ponnamp and K. Swarnasri, "Multi-Objective Optimal Allocation of Electric Vehicle Charging Stations and Distributed Generators in Radial Distribution Systems using Metaheuristic Optimization Algorithms," *Engineering, Technology & Applied Science Research*, vol. 10, no. 3, pp. 5837–5844, Jun. 2020, <https://doi.org/10.48084/etasr.3517>.
- [2] T. L. Duong and T. T. Nguyen, "Network Reconfiguration for an Electric Distribution System with Distributed Generators based on Symbiotic Organisms Search," *Engineering, Technology & Applied Science Research*, vol. 9, no. 6, pp. 4925–4932, Dec. 2019, <https://doi.org/10.48084/etasr.3166>.
- [3] P. Balamurugan, T. Yuvaraj, and P. Muthukannan, "Optimal Allocation of DSTATCOM in Distribution Network Using Whale Optimization Algorithm," *Engineering, Technology & Applied Science Research*, vol. 8, no. 5, pp. 3445–3449, Oct. 2018, <https://doi.org/10.48084/etasr.2302>.
- [4] R. Małkowski, M. Izdebski, and P. Miller, "Adaptive Algorithm of a Tap-Changer Controller of the Power Transformer Supplying the Radial Network Reducing the Risk of Voltage Collapse," *Energies*, vol. 13, no. 20, Jan. 2020, Art. no. 5403, <https://doi.org/10.3390/en13205403>.
- [5] A. N. Hasan and N. Tshivhase, "Voltage regulation system for OLTC in distribution power systems with high penetration level of embedded generation," *International Transactions on Electrical Energy Systems*, vol. 29, no. 7, 2019, Art. no. e12111, <https://doi.org/10.1002/2050-7038.12111>.
- [6] A. Del Pizzic, L. Di Noia, D. Lauria, M. Crispino, A. Cantiello, and F. Mottola, "Control of OLTC distribution transformer addressing voltage regulation and lifetime preservation," in *2018 International Symposium on Power Electronics, Electrical Drives, Automation and Motion (SPEEDAM)*, Amalfi, Italy, Jun. 2018, pp. 1002–1007, <https://doi.org/10.1109/SPEEDAM.2018.8445294>.
- [7] N. Tshivhase, A. N. Hasan, and T. Shongwe, "A Fault Level-Based System to Control Voltage and Enhance Power Factor Through an On-Load Tap Changer and Distributed Generators," *IEEE Access*, vol. 9, pp. 34023–34039, 2021, <https://doi.org/10.1109/ACCESS.2021.3061622>.
- [8] K. Kotsalos, I. Miranda, J. L. Dominguez-Garcia, H. Leite, N. Silva, and N. Hatziaargyriou, "Exploiting OLTC and BESS Operation Coordinated with Active Network Management in LV Networks," *Sustainability*, vol. 12, no. 8, Jan. 2020, Art. no. 3332, <https://doi.org/10.3390/su12083332>.
- [9] D. F. Teshome, W. Xu, P. Bagheri, A. Nassif, and Y. Zhou, "A Reactive Power Control Scheme for DER-Caused Voltage Rise Mitigation in Secondary Systems," *IEEE Transactions on Sustainable Energy*, vol. 10,

- no. 4, pp. 1684–1695, Jul. 2019, <https://doi.org/10.1109/TSTE.2018.2869229>.
- [10] A. A. Firdaus, "Optimasi On-Load Tap-Changing Menggunakan Quantum Differential Evolution Untuk Meminimalkan Kerugian Daya," *Jurnal ELTIKOM: Jurnal Teknik Elektro, Teknologi Informasi dan Komputer*, vol. 2, no. 1, pp. 9–17, Jun. 2018, <https://doi.org/10.31961/eltikom.v2i1.43>.
- [11] G. Wenjie, Y. Litao, H. Aoyang, and L. Zhengjie, "Optimal Dispatch Model of Active Distribution Network Based on Particle Swarm optimization Algorithm with Random Weight," in *2021 IEEE 2nd International Conference on Big Data, Artificial Intelligence and Internet of Things Engineering (ICBAIE)*, Nanchang, China, Mar. 2021, pp. 482–485, <https://doi.org/10.1109/ICBAIE52039.2021.9389910>.
- [12] P. R. Chinda and R. Dalapati Rao, "A binary particle swarm optimization approach for power system security enhancement," *International Journal of Electrical and Computer Engineering (IJECE)*, vol. 12, no. 2, Apr. 2022, Art. no. 1929, <https://doi.org/10.11591/ijece.v12i2.pp1929-1936>.
- [13] N. A. Nguyen, T. N. Le, and H. M. V. Nguyen, "Multi-Goal Feature Selection Function in Binary Particle Swarm Optimization for Power System Stability Classification," *Engineering, Technology & Applied Science Research*, vol. 13, no. 2, pp. 10535–10540, Apr. 2023, <https://doi.org/10.48084/etasr.5799>.
- [14] S. Tu, O. U. Rehman, S. U. Rehman, S. Ullah, M. Waqas, and R. Zhu, "A Novel Quantum Inspired Particle Swarm Optimization Algorithm for Electromagnetic Applications," *IEEE Access*, vol. 8, pp. 21909–21916, 2020, <https://doi.org/10.1109/ACCESS.2020.2968980>.
- [15] Y. Wang and X. Chen, "Hybrid quantum particle swarm optimization algorithm and its application," *Science China Information Sciences*, vol. 63, no. 5, May 2020, Art. no. 159201, <https://doi.org/10.1007/s11432-018-9618-2>.
- [16] C. Li, M. Shi, Y. Zhou, and E. Wang, "Quantum Particle Swarm Optimization Extraction Algorithm Based on Quantum Chaos Encryption," *Complexity*, vol. 2021, no. 1, 2021, Art. no. 6627804, <https://doi.org/10.1155/2021/6627804>.
- [17] M. Kamel, A. A. Karrar, and A. H. Eltom, "Development and Application of a New Voltage Stability Index for On-Line Monitoring and Shedding," *IEEE Transactions on Power Systems*, vol. 33, no. 2, pp. 1231–1241, Mar. 2018, <https://doi.org/10.1109/TPWRS.2017.2722984>.
- [18] D. Hamid and N. Gupta, "Stability Improvement of Power System with Wind Integration based on L-index," in *2021 Innovations in Power and Advanced Computing Technologies (i-PACT)*, Kuala Lumpur, Malaysia, Nov. 2021, pp. 1–6, <https://doi.org/10.1109/i-PACT52855.2021.9696900>.
- [19] A. A. Firdaus, O. Penangsang, A. Soeprijanto, and D. F. U.p, "Distribution Network Reconfiguration Using Binary Particle Swarm Optimization to Minimize Losses and Decrease Voltage Stability Index," *Bulletin of Electrical Engineering and Informatics*, vol. 7, no. 4, pp. 514–521, Dec. 2018, <https://doi.org/10.11591/eei.v7i4.821>.
- [20] A. Azizvahed *et al.*, "Energy Management Strategy in Dynamic Distribution Network Reconfiguration Considering Renewable Energy Resources and Storage," *IEEE Transactions on Sustainable Energy*, vol. 11, no. 2, pp. 662–673, Apr. 2020, <https://doi.org/10.1109/TSTE.2019.2901429>.
- [21] A. Al-Sakkaf and M. AlMuhaini, "Power Flow Analysis of Weakly Meshed Distribution Network Including DG," *Engineering, Technology & Applied Science Research*, vol. 8, no. 5, pp. 3398–3404, Oct. 2018, <https://doi.org/10.48084/etasr.2277>.
- [22] Q. Wu, Y. Shen, Z. Ma, J. Fan, and R. Ge, "iBQPSO: an Improved BQPSO Algorithm for Feature Selection," in *2018 International Joint Conference on Neural Networks (IJCNN)*, Rio de Janeiro, Brazil, Jul. 2018, pp. 1–8, <https://doi.org/10.1109/IJCNN.2018.8489676>.
- [23] S. Kumar Sahoo, E. H. Houssein, M. Premkumar, A. Kumar Saha, and M. M. Emam, "Self-adaptive moth flame optimizer combined with crossover operator and Fibonacci search strategy for COVID-19 CT image segmentation," *Expert Systems with Applications*, vol. 227, Oct. 2023, Art. no. 120367, <https://doi.org/10.1016/j.eswa.2023.120367>.
- [24] S. Chakraborty, A. K. Saha, and A. Chhabra, "Improving Whale Optimization Algorithm with Elite Strategy and Its Application to Engineering-Design and Cloud Task Scheduling Problems," *Cognitive Computation*, vol. 15, no. 5, pp. 1497–1525, Sep. 2023, <https://doi.org/10.1007/s12559-022-10099-z>.
- [25] S. Sharma, A. K. Saha, S. Roy, S. Mirjalili, and S. Nama, "A mixed sine cosine butterfly optimization algorithm for global optimization and its application," *Cluster Computing*, vol. 25, no. 6, pp. 4573–4600, Dec. 2022, <https://doi.org/10.1007/s10586-022-03649-5>.
- [26] S. Chakraborty, A. K. Saha, S. Sharma, S. K. Sahoo, and G. Pal, "Comparative Performance Analysis of Differential Evolution Variants on Engineering Design Problems," *Journal of Bionic Engineering*, vol. 19, no. 4, pp. 1140–1160, Jul. 2022, <https://doi.org/10.1007/s42235-022-00190-4>.
- [27] S. Sharma, A. K. Saha, A. Majumder, and S. Nama, "MPBOA - A novel hybrid butterfly optimization algorithm with symbiosis organisms search for global optimization and image segmentation," *Multimedia Tools and Applications*, vol. 80, no. 8, pp. 12035–12076, Mar. 2021, <https://doi.org/10.1007/s11042-020-10053-x>.